

# Design of a 3D-Printed Soft Robot with Posture and Steering Control

Takuya Umedachi<sup>1</sup> and Barry A. Trimmer<sup>2</sup>

**Abstract**—Both postural maintenance and rhythm generation are keys to generating adaptive behavior in all animals. This is particularly evident in soft animals such as caterpillars, worm and flatworms that are capable of moving freely in all directions and adopting intricate postures. They can also exploit three-dimensional deformations and nonlinear structural properties to move in complex environments and to respond to external forces. These capabilities have inspired a new interest in using soft materials in robotic applications but highly deformable materials create significant design and control problems. In previous work the authors have developed a 3D-printed soft (3D-PS) robot, inspired by caterpillars, as a platform to investigate methods for controlling soft robots. The previous version of the robot is able to reproduce the different gait patterns (inching and crawling motion) of caterpillars by changing temporal difference in the rhythmic deformations of different body parts. In this paper, we have added posture control to the 3D-PS robot together with a steering capability. Experimental results show that although posture and steering are usually related, elastic and continuum properties of the soft body can produce more complex and versatile behaviors.

## I. INTRODUCTION

Animals are mainly composed of soft and rheologically complex materials such as muscles, tendons, and layers of skin-like tissues. Because of these soft mechanical properties, animals are capable of storing elastic energy, cushioning the shock, and conforming to complex shapes in the environment. This is in sharp contrast to traditional rigid-body robots and is expected to be a key factor in generating adaptive behaviors in uncertain and dynamically changing environments. Inspired by the difference between machines and animals, many roboticists have paid a lot of attention to soft robotics (e.g., locomotion of caterpillars and worms, manipulation of octopus arm and elephant trunk [1], [2], [3], [4], [5], [6]). An important principle in the design of soft robots is that they need to implement morphological computation [7], [8] or active sensing [9] to exploit the large deformability and non-linearity of the soft body. Such robots are expected to exceed the limitations of traditional hard and rigid robotic systems. The challenge, however, remains to design and control the soft body effectively.

Animal locomotion involves two important control mechanisms: postural maintenance and rhythm generation. These

<sup>1</sup>T. Umedachi is research fellow of the Japan Society for the Promotion of Science and research fellow of Japan Science and Technology Agency (JST) CREST at Tufts University, Medford MA 02155, USA and Hiroshima University, 1-3-1 Kagamiyama, Higashi-hiroshima 7398526, JAPAN. takuya.umedachi at gmail.com

<sup>2</sup>B. A. Trimmer is Henry Bromfield Pearson Professor of Natural Sciences and Director of Neuromechanics and Biomimetic Devices Laboratory at Tufts University, Medford MA 02155, USA barry.trimmer at tufts.edu

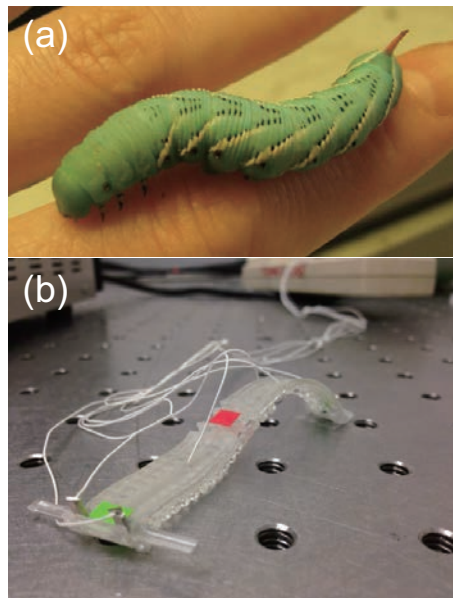


Fig. 1. (a) Model animal of soft robot, *Manduca sexta* and (b) new steering model of Printed Soft robot (PS robot) proposed.

two controls are universal from lower forms of life (e.g., caterpillars, worm, flatworm) to human beings [10], [11], [12]. Actually, combining these controls on soft bodies allows animals to generate surprisingly adaptive behavior in three-dimensional space; not only can these bodies stretch or compress they can also bend, wrinkle, buckle, twist, droop, and creep along or against complex environment. Furthermore, the viscoelastic properties of tissues produces different mechanical responses at different strain rates, which enables the body to respond differently as it interacts with external forces from the environment. These interactions are also affected by the body configuration, which in soft animals can change dramatically with different postures. Hence, it is necessary to develop a control system for soft robots in which rhythm generation and posture maintenance are well coordinated to exploit viscoelastic and continuum properties of soft bodies.

Thus far, we have developed a 3D-printed soft (3D-PS) robot [13] inspired by a highly deformable and relatively simple-shape animal, the caterpillar (*Manduca sexta*). We successfully demonstrated that the elastic and continuum nature of soft robots makes it possible to create waves of deformation along the body to generate two different gaits (inching and crawling) even using a small number of actuators. Furthermore, these large deformations can be

exploited to change frictional interactions with the substrate during each step by bringing different materials into contact with the environment. However, locomotion of the robot is limited to forward and backward movement since the control system only focuses on the rhythm generation.

The paper presents a new version of the 3D-PS robot (Figure 1(b)) that is able to steer during the locomotion. Key aspects for designing the soft robot are as follows: 1) well coordinated deformation control including both left-right and up-down bending; 2) locomotion capability exploiting the up-down deformation of the body so as to reproduce the two different locomotion gaits; 3) exploiting the dynamic responses (e.g., viscoelastic and continuum properties) of soft materials to induce nontrivial and versatile behaviors. The experimental results shows that exploiting complex mechanical dynamics of soft materials (i.e., viscoelastic and continuum deformation) allows simple control to promote adaptive and versatile behaviors. The results can also contribute to an understanding of how a living system generates versatile and adaptive behaviors with morphological computation [8] of their bodies, in the sense that viscoelastic and continuum deformation of soft materials can reduce, or take over, some of the processes usually attributed to control.

The remainder of this paper is organized as follows. Section II introduces the PS robot and presents a description of its mechanical and control systems, which enable it to move freely in all directions exploiting three dimensional deformation of the body. Section III then presents some of the important data obtained by the experiments. Finally, section IV presents the conclusions and recommendations for future work.

## II. SOFT ROBOT DESIGN

### A. Mechanical design for steering

The new version of 3D-PS robot is presented in Figure 2, which consists of a soft body with variable friction legs and three coiled shape memory alloys (SMAs). The body is printed using multi-material printable 3-D printer (Objet Connex 500, 3-D printer) with two materials. One is soft rubber-like Objet TangoPlus. Another is hard polypropylene-like Objet VeroClear\*. The structure with blocks aligned in a straight line on the ventral side (see Figures 2(c), (e)) has holes along the straight line to guide SMA coil inside and allows the SMA coil to cool quickly. On the middle of the dorsal side, the zigzag structure is designed (see Figure 2(d)) as so-called a joint part on the soft body, which makes it easy to bend right-left for steering purpose.

The SMA coils (18 mm in compressed condition, BMX100, Toki Corporation)<sup>†</sup> are tactfully embedded in the structures and are electrically actuated. In particular, as shown in Figure 2(c), three SMA coils were arranged side-

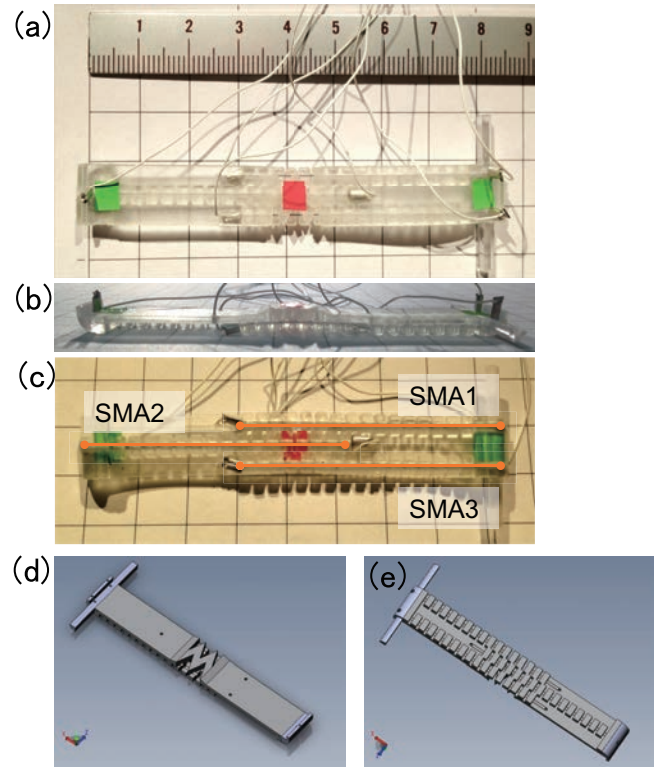


Fig. 2. (a) Top view of the robot. (b) Side view of the robot. (c) Bottom view and arrangement of the three SMAs inside robot body. One square is 1 cm x 1 cm in (a)-(c). The SMA coils are embedded overlapped along the body axis. (d) Bird's eye view of the cad data (the ventral side is top). (e) Bird's eye view of the cad data (the dorsal side is top).

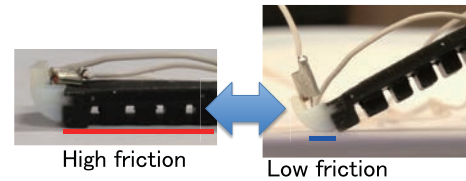


Fig. 3. Side view of variable friction leg design. For description of the mechanism, the leg was printed with white material instead of VeroClear as hard part, and black material instead of TangoPlus as soft part in this figure. Red line indicates high friction surface with the soft part and blue line indicates low friction contact point with the hard part.

by-side and overlapped<sup>‡</sup>. Two SMA coils are located on the rear part and one SMA coil is located on the front part. This overlapped SMA alignment design allows for the robot both to send up-down bending wave from one part to another (i.e., from rear to front to move forward or front to rear to move backward). In addition to this, the antagonistic SMA alignment design enables to bend left and right around the joint part.

### B. Variable friction legs

Based on the previous version of PS robot [13], variable friction legs are designed to switch friction with the ground

<sup>‡</sup>Each end of each SMA are connected with electric cable with a crimping terminal.

\*The mechanical properties of the materials are found in the following url: <http://www.stratasys.com>.

<sup>†</sup>The detail information of the SMA coils is found in the following url: <http://www.toki.co.jp/biometal/english/contents.php>.

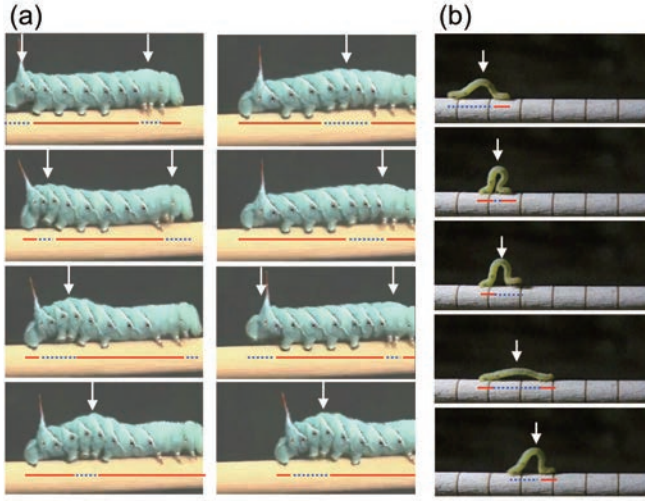


Fig. 4. (a) Crawling locomotion gait and (b) inching locomotion gait. The blue broken lines indicate lifted-up parts of the body whereas the red solid lines indicate gripping parts of the body. The arrows indicate peaks of the bending wave of the body. Since the arrow/arrows moving direction and locomotion direction are the same, direct wave is confirmed in the both locomotion gaits.

for locomotion. The proposed design, as shown in Figure 3, uses two materials: TangoPlus (see-through rubber-like substance) and VeroClear (see-through hard substance). The TangoPlus has higher friction coefficient than VeroClear. Use of materials with two different friction coefficients allows the robot to switch friction with the ground on an edge of the robot by bending the body (see Figure 3). This friction switch mechanism allows the front/rear part to slip with the substrate and start the direct wave for locomotion. We printed the robot see-through materials for putting marks to measure the positions of the markers.

### C. Gait Generation

There are two types of locomotion on caterpillars (depending on species, body weights, and positions of prolegs): inching and crawling gaits (see Fig. 4). With regard to the both locomotion gaits, it is important to control and generate up-down bending wave that starts from the rear part and moves forward along the body (i.e., direct wave). Inching gait is a modal wave with its wavelength almost equal to the body length, whereas crawling gait is a modal wave with its wavelength approximately half of the body length or less than that. In order to reproduce the caterpillar locomotion gaits on the caterpillar-like soft robot, we used two SMA coils in our previous study and focused on phase difference (i.e., time difference) of firings between the two SMA coils<sup>§</sup>, and successfully generated inching and crawling motion by changing the phase difference. (Please go to <https://www.youtube.com/watch?v=0pHOaBnj1po> to see the digest movie of [13].)

<sup>§</sup>Of course, the other variables are available for designing the actuation signals such as amplitude of the SMA actuators (voltage applied across the SMA), frequency of actuation of SMA, and wavelength of SMA actuation signal (decided by SMA coil arrangement).

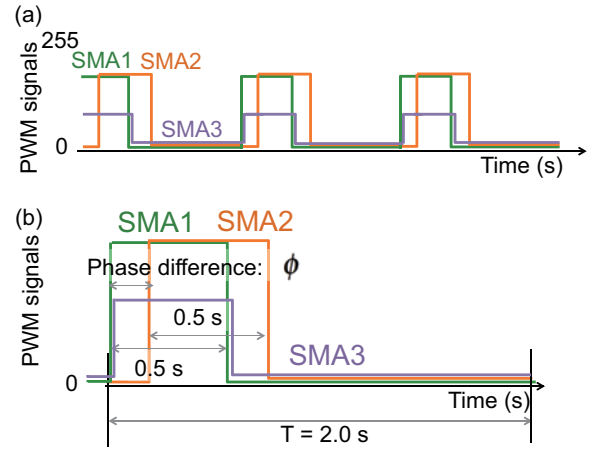


Fig. 5. (a) Example of PWM signals generated by the microcomputer, and (b) one period of the signal. Here, SMA1, SMA2, and SMA3 denote the SMA coils described earlier in Figure 2. The time period  $T$  is fixed at 2 s, and the actuation time is fixed 0.5 s. The phase difference  $\phi$  denotes the difference in time between actuation in front part (SMA1 and SMA3) and in rear part (SMA2). In order to bend right and left for steering purpose, on-state PWM values between SMA1 and SMA3 can be different.

In this paper, in order to build a steering model of the soft robot, three SMA coils are embedded on the body. The two SMA coils on the rear part (i.e., SMA1 and SMA3) generate up-down bending motion and lift up the body part. One example of PWM signals to three SMA coils is illustrated in Figure 5. By changing on-state PWM values between SMA1 and SMA3, right-left bending around the joint part can be achieved easily, which makes it possible to steer. After the phase difference, the SMA coil on the front part (i.e., SMA2) generates up-down bending motion, and the deformation on the rear part shifts to the front part when the phase difference is relatively small.

Behavioral change between inching and crawling depends on how much deformation is generated per a fixed time. The parameters can be phase difference, force of SMA coils, and viscoelastic properties of the soft material. The previous study demonstrated that inching gait is generated when the phase difference is less than 0.2 s and crawling gait is generated when the phase difference is more than 0.2 s [13]. However, even setting phase difference 0.3 s in the previous model, crawling motion is expected to change to inching motion when electric current (which is governed with PWM signal) to SMA coils is increased. Larger deformation is slowly resolved due to the damping properties of the soft materials. In this paper, we set 0.3 s as phase difference since the crawling-inching behavioral change is expected by changing PWM signals to SMA coils.

In order to realize such control system, we built open loop control for the robot. The circuit board consists of one Arduino Uno (Arduino, 2012) and three motor drivers (TA7291P, Toshiba Co.) as shown in Figure 6. The Arduino Uno was programed to generate PWM signals as input signals to each motor drivers. Each motor driver switches on and off external power supply (7 V) to each SMA embedded



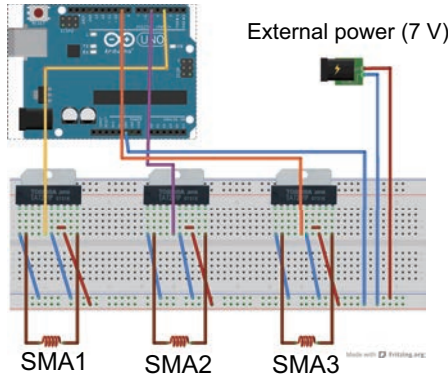


Fig. 6. Circuit board consisting of Arduino Uno and three motor drivers as control system for the soft robot.

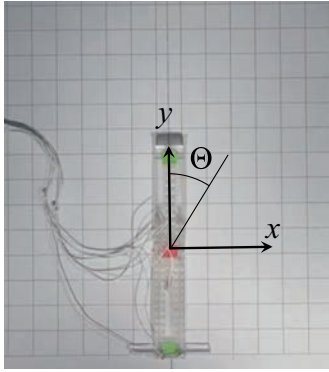


Fig. 7. Photograph of experimental setup. The robot is placed on a flat paper. One square is 1 cm x 1 cm.

in the robot. The time period of the SMA actuation signal is set to 2 s<sup>‡</sup>.

### III. EXPERIMENT

#### A. Experimental setup

To evaluate the validity of this new 3D-PS robot capable of steering, we recorded the behavior of the robot changing value of PWM values for SMA1 and SMA3 when  $\phi = 0.3$  s. Here, PWM1, PWM2, and PWM3 denote on-state PWM values of SMA1, SMA2, SMA3, respectively (see Figure 5 as one example). PWM2 is fixed to 180 during the all trials. As can be seen in Figure 7, the robot was placed on a paper (letter size) positioned on a flat substrate, and programmed to generate locomotion for 20 s (i.e., 10 periods). The experiment was conducted in room temperature. The trajectories of the center of the robot were recorded and, both the distance traveled and angle of body configuration after 20 s, were measured. In order to measure these values, three markers were put on the front, center, and rear part on the dorsal side of the robot.

<sup>‡</sup>Although the SMA coils have muscle-like properties, they do have limitations as robotic actuators: their maximum actuation frequency is limited by their cooling time. Due to this, we set one cycle time as 2 s for cooling SMA coils, which seems to be sufficiently long, as we look the motion (see the attached movie).

#### B. Experimental Results

Figure 8 represents the trajectories of the robot when values of PWM1 and PWM3 are changed. Please note that value of PWM3 is always not more than value of PWM1. This elimination is due to the symmetry of the body structure. When the values of PWM1 and PWM3 are the same, the robot generates forward locomotion. By setting PWM value of SMA3 is 0, the robot steers right. When value of PWM3 is increased, the robot changes the direction to go. This shows that the robot has the capability of steering. Interestingly, when PWM1 is 250 and PWM3 is 200, the robot is steering 'left' even though the value of PWM3 is less than the value of PWM1.

Figure 9 represents distance traveled after 20 s, which are calculated with data of the trajectories. As can be seen in the figure, two data (PWM1=200, PWM3=200 and PWM1=250, PWM3=200) are much higher than the rest. This difference is caused by inching locomotion gaits, i.e., the robot can move faster with inching motion than with crawling motion (see the attachment video file). This indicates that the amount of electric current to SMA coils per a fixed time changes the locomotion gait.

Figure 10 illustrates steering angle after 20 s, which are calculated with data of the trajectories. Here the steering angle  $\Theta$  is defined as

$$\Theta = \arctan\left(\frac{x(t=20) - x(t=0)}{y(t=20) - y(t=0)}\right), \quad (1)$$

based on the angle definition in Figure 7. In order to confirm the controllability of the steering angle along the unbalance between SMA1 and SMA3, we employed (PWM1-PWM3)/PWM1 as the horizontal axis. As can be seen in the figure, steering angle can be controlled when combination of PWM1 and PWM3 is appropriate.

Figure 11 shows angle of body configuration after 20 s when values of PWM1 and PWM3 are changed. The angle is measured with green two markers on the front and rear dorsal sides of the body in Figure 2. When comparing Figure 8 and Figure 11, the angle of body configuration and steering angle can be different (in some data they are opposite). For example, the robot is able to rotate counterclockwise (left) on the spot when SMA1 = 150, SMA3 = 50 (see the video attachment). Another example is SMA1 = 250, SMA3 = 100; the robot moves right but the body rotates left (see the video attachment). These experimental results indicate that the robot exhibits very complex behaviors according to the combination of the PWM values on the SMA coils in the rear part.

### IV. CONCLUSION AND FUTURE WORK

We have presented a new steering version of highly deformable 3-D PS robot. The soft body is designed in ways that not only bends up-down to achieve direct wave for locomotion but also bends right and left to steer. The right-left bending is controllable by supplying unequal current to antagonistic SMA coils on the rear part. The experimental results show that the robot is able to generate versatile

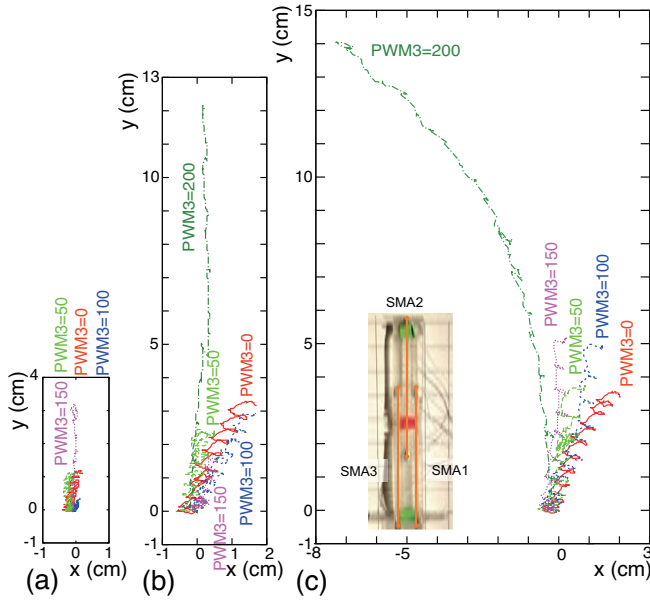


Fig. 8. Trajectories of the center of the robot (red marker on the dorsal side in Figure 2) during 20 s when changing PWM values for SMA1 and SMA3. (a) Trajectories when PWM1 is fixed to 150 and PWM3 value is changed. (b) Trajectories when PWM1 is fixed to 200 and PWM3 value is changed. (c) Trajectories when PWM1 is fixed to 250 and PWM3 value is changed.

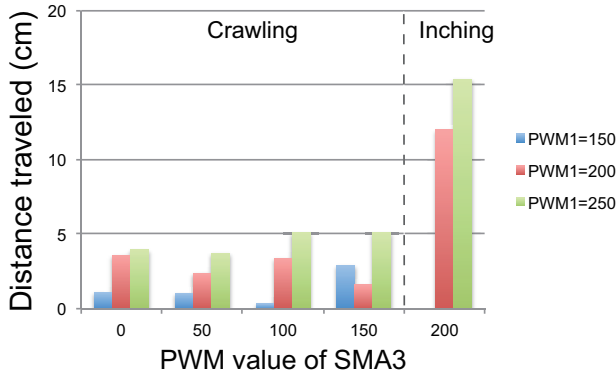


Fig. 9. Distance traveled of the center of the robot (red marker on the dorsal side in Figure 2) after 20 s when changing PWM values for SMA1 and SMA3.

locomotion in a complex environment, e.g., rotating on the spot and moving right with left rotation. Furthermore, data from our experiment provide preliminary evidence that the dynamics of the mechanical system (i.e. the viscoelasticity and continuum properties of the soft robot) can be exploited so as to embed complex computations into the robot morphology and obtain versatile behaviors (i.e., steering and rotating) and useful function (i.e., friction control in this case). It should also be noted that the behaviors and function can be achieved with simple actuation of a few actuators. In addition, we believe that this robotic system can contribute to an understanding of how a living system generates supple, versatile, and adaptive behaviors with their complex and soft

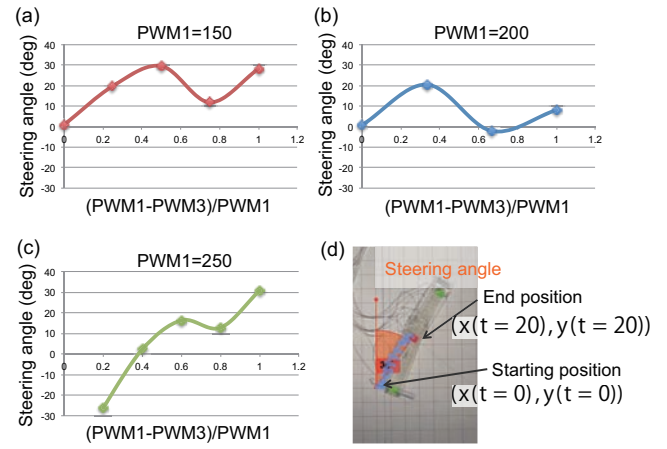


Fig. 10. Steering angle when PWM1 and PWM3 are changed. The angle is calculated with the starting and end positions. Right rotation is set as positive.



Fig. 11. Angle of body configuration after 20 s when changing on-state PWM values for SMA1 and SMA3. The value is measured with green two markers on the dorsal side in Figure 2. Right rotation is set as positive.

physical properties of their body, because the parameters (i.e. its viscoelastic parameters and body shapes) of the robotic system can be easily designed and changed. The fabrication of the robot was easy, quick, and economically cheap, thus, allowing fabrication in large numbers with ease.

The successful display of morphological computation in soft robots opens gates for greater research in design of soft robots that are capable of locomotion which includes climbing on a slop or tree branches. To do so, the optimal design of the legs for locomotion needs to be explored. Using tethers/strings (winded/un-winded by motors) instead of SMAs can be an alternative mechanical design especially for designing bigger soft robots. The behavior of the robot is strongly dependent on the viscoelastic properties of the body: the waves of deformation were damped by the resilience of soft material used for the chassis. It is assumed that changing the material properties (e.g., extensibility, elastic modulus, and viscoelasticity) will have a major effect on the realization of some functionalities.

It is also desired to explore how sensors can be embedded into the robot so as to maintain the soft, complex nature of the robot. For instance, embedding mechano-sensory

oscillator system [14] may allow the soft body parts to interact each other, which in turn generates reasonable and adaptive behaviors according to the physical properties of the body and environment. The modeling of such robots as deformable and continuum structures and other tools needs are to be explored. In parallel, 3-dimensional measurement of the behavior will be needed to compare the numerical data and experimental data. This will be beneficial to obtain richer information about the robot, in complex environments and building simulation platforms for better robot design. Finally, the variation of design parameters (e.g., placement of SMA coils, actuation voltage, etc.) also needs to be explored.

#### ACKNOWLEDGMENT

The authors would like to acknowledge the members of the Neuromechanics and Biomimetic Devices Laboratory in Department of Biology, Tufts University for their feedback. This research is partially supported by the Tateishi Science and Technology Foundation (No. 2021005) and NSF Award (DBI-1126382).

#### REFERENCES

- [1] S. Kim, C. Laschi, and B. Trimmer. Soft robotics: a bioinspired evolution in robotics. *Trends in Biotechnology* 31, 287-294, 2013.
- [2] M. W. Hannan and I. D. Walker. Kinematics and the implementation of an elephant's trunk manipulator and other continuum style robots. *Journal of Robotic Systems*, 20(2):45-63, 2003.
- [3] C. Laschi, M. Cianchetti, B. Mazzolai, L. Margheri, M. Follador, and P. Dario. Soft robot arm inspired by the octopus. *Advanced Robotics*, 26(7):709-727, 2012.
- [4] H. Lin, G. G. Leisk, and B. Trimmer. Goqbot: a caterpillar-inspired soft-bodied rolling robot. *Bioinspiration & biomimetics*, 6(2) 026007, 2011.
- [5] S. Seok, C. D. Onal, R. Wood, D. Rus, and S. Kim. Peristaltic locomotion with antagonistic actuators in soft robotics. In *Robotics and Automation (ICRA)*, 2010 IEEE International Conference on, pages 1228-1233, IEEE, 2010.
- [6] D. Trivedi, C. D. Rahn, W. M. Kier, and I. D. Walker. Soft robotics: Biological inspiration, state of the art, and future research. *Applied Bionics and Biomechanics*, 5(3):99-117, 2008.
- [7] R. Pfeifer and J. C. Bongard. *How the body shapes the way we think: a new view of intelligence*. MIT press, 2006.
- [8] R. Pfeifer, F. Iida, and G. Gómez. Morphological computation for adaptive behavior and cognition. *International Congress Series*, 1291, 22-29, 2006, doi:10.1016/j.ics.2005.12.080
- [9] K. Hosoda, Y. Yamasaki, and M. Asada. Sensing the texture of surfaces by anthropomorphic soft fingertips with multi-modal sensors. *Proceedings. 2003 IEEE/RSJ International Conference on (Volume:1)*, 1:31-35, 2003.
- [10] R. McNeill Alexander. *Exploring Biomechanics: Animals in Motion*. W H Freeman & Co, ISBN-13: 978-0716750352, 1992.
- [11] T. G. Deliagina and G. N. Orlovsky. Comparative neurobiology of postural control. *Current Opinion in Neurobiology*, 12, 6, pp. 652-657, 2002.
- [12] S. Grillner, O. Ekeberg, A. Manira, A. Lansner, D. Parker, J. Tegner and P. Wallen, Intrinsic function of a neuronal network —a vertebrate central pattern generator, *Brain Res. Rev.* 26, 184-197, 1998.
- [13] T. Umedachi, V. Viskas, and B. A. Trimmer. Highly Deformable 3-D Printed Soft Robot Generating Inching and Crawling Locomotions with Variable Friction Legs. *Proceedings. 2013 IEEE/RSJ International Conference on Intelligent Robots and Systems (IROS 2013)*, November 3-8, 2013.
- [14] T. Umedachi, R. Idei, K. Ito, and A. Ishiguro. True-slime-mould-inspired hydrostatically-coupled oscillator system exhibiting versatile behaviours, *Bioinspir. Biomim.*, 8, 035001, doi:10.1088/1748-3182/8/3/035001, IOP Publishing, 2013.